HOPX Is a ZNF750 Target that Promotes Late Epidermal Differentiation

Journal of Investigative Dermatology (2019) **139,** 2039–2042; doi:10.1016/j.jid.2019.03.1141

TO THE EDITOR

Homeodomain-containing proteins are broadly involved in regulating development and cell fate decisions (Bürglin and Affolter, 2016). The homeodomain-only protein (known as HOP or HOPX) is unique within this family of proteins due to its inability to bind DNA and is expressed abundantly in differentiated layers of the epidermis (Obarzanek-Fojt et al., 2011; Yang et al., 2010), suggesting a potential role for HOPX in epidermal differentiation. HOPX governs a balance between proliferation and differentiation in the heart (Chen et al., 2002), lungs (Yin et al., 2006), and muscle (Kee et al., 2007), but its role in epidermal homeostasis is controversial (Mariotto et al., 2016). In one study, experimental HOPX depletion in keratinocytes inhibited expression of filaggrin and transglutaminase-1, suggesting that it is required to promote differentiation (Obarzanek-Fojt et al., 2011). By contrast, a second study found that HOPX knockdown resulted in loricrin and involucrin up-regulation, whereas its overexpression in immortalized HaCaT keratinocytes repressed loricrin and involucrin (Yang et al., 2010). This conversely suggested that HOPX inhibits differentiation.

The uncertainty about HOPX function has important implications, because it has been identified as a key genetic determinant in epidermal differentiation (Lopez-Pajares et al., 2015) and psoriasis (Li et al., 2014). In this context, we sought to better define the role of HOPX in keratinocyte differentiation. We first aimed to place HOPX within the network of regulators that control epidermal development. To identify candidate regulatory enhancers near HOPX, we examined ENCODE data for histone 3, lysine 27 acetylation (H3K27Ac), and DNase-I hypersensitivity sites (DHSs) in neonatal human epidermal keratinocytes. A strong peak approximately 6 kilobases downstream of the 3′ end of HOPX showed coincident H3K27Ac and DHS enrichment (Figure 1a). We also examined chromatin immunoprecipitation-sequencing data with a focus on transcription factors active in skin. This identified a binding site for the transcription factor ZNF750 overlapping with the H3K27Ac/DHS peak. ZNF750 is a p63 target that promotes differentiation in human epidermis (Sen et al., 2012).

To evaluate if ZNF750 controls HOPX expression through binding of this enhancer, we first depleted ZNF750 using short hairpin RNA (shZNF750) and evaluated HOPX expression (Figure 1b and c). We used primary neonatal keratinocytes isolated from discarded surgical specimens with written informed patient consent, under approval of a University of California–San Diego institutional review board protocol. HOPX up-regulation was strongly inhibited by ZNF750 depletion, suggesting that ZNF750 is required for HOPX induction. We then overexpressed ZNF750 in keratinocytes grown in progenitor conditions. Overexpression of ZNF750 stimulated strong HOPX expression (Figure 1d). Viewed together, these experiments showed that ZNF750 is both necessary and sufficient for HOPX induction.

Next, we used clustered regularly-interspaced short palindromic repeats (i.e., CRISPR)/Cas9-mediated genomic editing to delete the candidate enhancer to determine if it was required for ZNF750 to control HOPX expression. Two single guide RNAs (sgRNAs) were designed to flank the ZNF750 genomic binding site (denoted as sgEnhancer) and infected into Cas9-expressing keratinocytes. PCR of genomic DNA was used to assess targeted deletion (Figure 1e). With this approach, the enhancer was deleted in approximately 75% of pooled keratinocytes (Figure 1f). We attempted multiple times to isolate individual sgEnhancer clones but could not propagate primary clones long enough to perform downstream experiments. Therefore, we compared pools of sgEnhancer keratinocytes against those infected with control sgRNAs (sgControl). Assessing HOPX mRNA induction, we found that HOPX mRNA induction was inhibited by approximately 50% in sgEnhancer keratinocytes (Figure 1g), consistent with this enhancer having a role in inducing HOPX expression. To further test whether ZNF750 binding was specifically involved with this enhancer element, we overexpressed ZNF750 in differentiating sgControl versus sgEnhancer keratinocytes. ZNF750 overexpression induced HOPX protein levels in sgControl cells but did not lead to higher expression in the sgEnhancer cells (Figure 1h). Together, these experiments show that HOPX is a downstream activation target of the transcription factor ZNF750, which acts, at least in part, through binding an enhancer downstream of HOPX.

These results indicated that HOPX lies within a genetic pathway known to activate keratinocyte differentiation. To further substantiate this result, we assessed the genome-wide transcriptional impact of depleting HOPX. Prior in vitro studies of HOPX used transfection of short interfering RNAs, which caused either incomplete and transient protein depletion (Obarzanek-Fojt et al., 2011) and/or were partially performed in immortalized HaCaT cells (Yang et al., 2010). To generate durable HOPX depletion in a primary cell and tissue context, we used stable short hairpin knockdown (shHOPX) in primary neonatal keratinocytes and

Abbreviations: DEG, differentially expressed gene; DHS, DNase-I hypersensitivity site; sgRNA, single guide RNA

Accepted manuscript published online 5 April 2019; corrected proof published online 22 May 2019

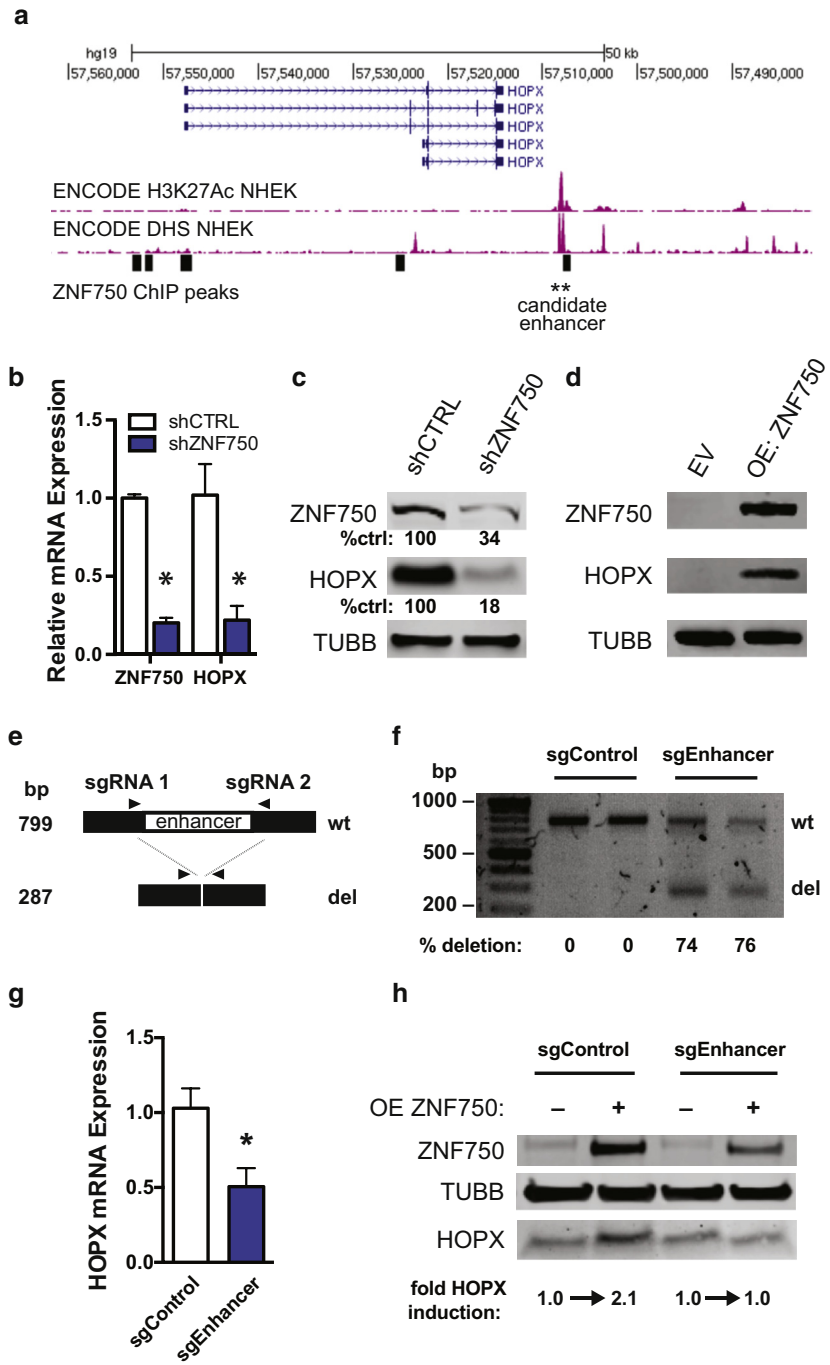

Figure 1. HOPX is induced by ZNF750 binding at a downstream enhancer. (**a**) Chromatin immunoprecipitation-sequencing tracks around the HOPX genomic locus. ZNF750 binding sites are represented as black rectangles. (**b**) qRT-PCR of control and ZNF750-depleted (shZNF750) keratinocytes differentiated for 6 days. n = 2. Error bars show standard error of the mean. $*P < 0.05$. (**c**) Western blot of day 5 differentiated keratinocytes after short hairpin RNA-induced depletion of ZNF750 (shZNF750). Quantitation of band intensity performed with Li-Cor software (Li-Cor, Lincoln, NE). Band intensities were normalized to loading control and shCTRL band intensity. (**d**) Western blot of keratinocytes transduced to overexpress ZNF750 (OE ZNF750). Keratinocytes were infected with empty vector or ZNF750-HA. (**e**) Scheme of CRISPR/Cas9-mediated enhancer deletion and detection by PCR assay. (**f**) PCR assay to detect HOPX enhancer deletion. Cas9 was introduced into keratinocytes along with sgRNAs flanking the candidate enhancer (sgEnhancer) or scramble control guides (sgControl). Quantitation of band intensity was performed with Bio-Rad (Hercules, CA) Image Lab software analysis. Band intensities were normalized to amplicon length to determine relative deletion efficiency. (**g**) qRT-PCR of HOPX expression in control and enhancer-deleted pooled differentiated keratinocytes. n = 3. Error bars show standard error of the mean. $*P < 0.05$. (**h**) Western blot of differentiating sgControl and sgEnhancer keratinocytes transduced to overexpress ZNF750. Quantification was performed with LiCor software. bp, base pair; ChIP, chromatin immunoprecipitation; ctrl, control; CRISPR, clustered regularly-interspaced short palindromic repeats; del, deletion; DHS, DNase hypersensitivity site; EV, empty vector; H3K27Ac, histone 3, lysine 27 acetylation; kb, kilobase; NHEK, normal human epidermal keratinocyte; OE, overexpression; qRT-PCR, quantitative real-time reverse transcriptase–PCR; sg, single guide; sh, short hairpin; wt, wild type.

regenerated organotypic epidermal tissue. Stable knockdown depleted HOPX mRNA by 98.4% ± 0.1% (mean ± standard error of the mean, n = 3) compared with the control (shCTRL) and reduced HOPX to undetectable levels on Western blot (Figure 2a).

We performed whole-transcriptome sequencing of shCTRL and shHOPX keratinocytes differentiated for 6 days in vitro (data available at National Center for Biotechnology Information Gene Expression Omnibus no. GSE125152). Using a threshold of 2-fold expression change and an analysis of variance/false discovery rate of less than 0.01, HOPX depletion resulted in 589 differentially expressed genes (DEGs) (Figure 2b). Gene Ontology analysis with PANTHER classification (Mi et al., 2013) showed strong enrichment for genes involved with cornification and keratinocyte differentiation (Figure 2c). To confirm these results, we validated the expression of key differentiation-related transcripts using quantitative real-time reverse transcriptase–PCR and a second unrelated HOPX-targeting hairpin RNA (shB_HOPX) (Figure 2d). HOPX depletion did not significantly affect early differentiation transcripts keratin 1 and keratin 10 but repressed the late epidermal differentiation genes loricrin and late cornified envelope 3D (LCE3D). To evaluate this phenotype in a three-dimensional tissue context, we regenerated human epidermal tissue with shCTRL and shHOPX keratinocytes. Concordant with quantitative real-time

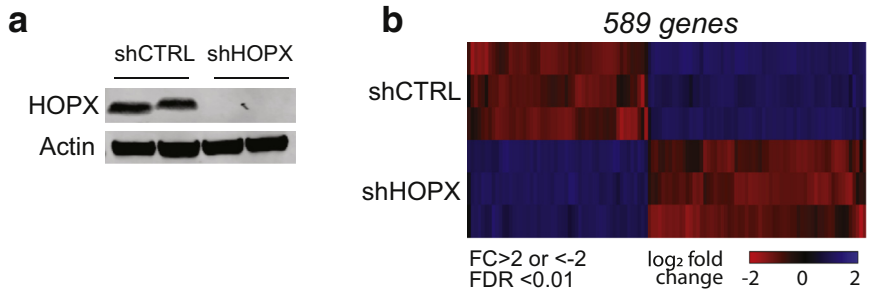

c

GO Term	# of genes	Bonferroni corrected p-value
cornification	23	1.1×10^{-8}
keratinocyte differentiation	30	4.1×10^{-6}
keratinization	26	3.3×10^{-5}
epidermal cell differentiation	30	1.0×10^{-4}

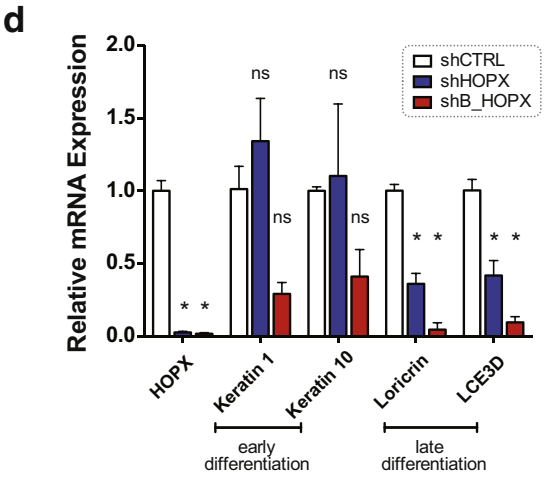

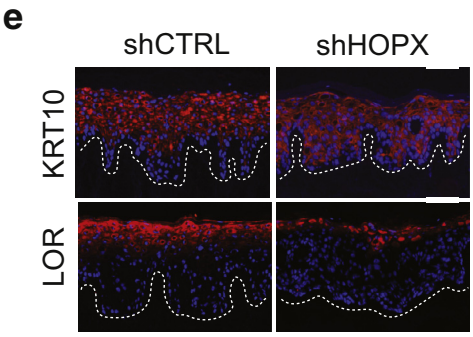

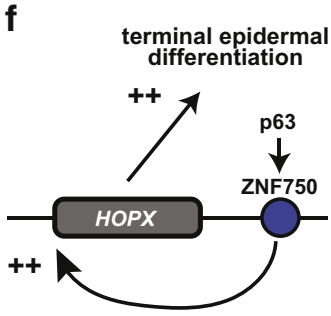

Figure 2. Depletion of HOPX inhibits late epidermal differentiation. (**a**) Western blot after shRNA-induced depletion of HOPX (shHOPX). (**b**) RNA sequencing of HOPX-depleted keratinocytes. Heatmap representing the differentially expressed genes (DEGs) associated with HOPX depletion. DEG threshold was assigned as fold change greater than 2 or less than −2, with a calculated false discovery rate of less than 0.01. (**c**) Gene Ontology enrichment analysis of DEGs altered by HOPX depletion with PANTHER classification. (**d**) qRT-PCR of differentiation-associated transcripts with HOPX depletion using two independent shRNAs against HOPX. n = 3. Error bars show standard error of the mean. *$P < 0.05$. ns = not significant. (**e**) Immunofluorescence staining of control and HOPX-depleted regenerated epithelial tissue. (**f**) Model of genetic p63-ZNF750-HOPX relationship in terminal keratinocyte differentiation. CTRL, control; FC, fold change; FDR, false discovery rate; GO, Gene Ontology; ns, not significant; qRT-PCR, quantitative real-time reverse transcriptase—PCR; sh, short hairpin.

reverse transcriptase—PCR results, protein expression of keratin 10 (KRT10) was unchanged, whereas expression of the terminal differentiation protein, loricrin (LOR), was diminished with HOPX knockdown (Figure 2e). Taken together, these data confirm that HOPX is a positive regulator of epidermal late differentiation.

In summary, these results show that HOPX functions downstream of ZNF750, a well-defined transcription factor in the skin that is activated by p63 (Sen et al., 2012). In this context, we propose that HOPX functions within a p63-ZNF750-HOPX pathway to upregulate the key proteins required for terminal epidermal differentiation (Figure 2f), providing clarity to previous studies showing conflicting results. Future studies will aim to decipher the molecular pathways and mechanisms operating downstream of HOPX that engage the late differentiation program.

Data availability statement

Data sets related to this article can be found at https://www.ncbi.nlm.nih.gov/geo/query/acc.cgi?acc=GSE125152, hosted at the National Center for Biotechnology Information Gene Expression Omnibus under accession no. GSE125152.

ORCIDs

Selena Y. Chen: https://orcid.org/0000-0001-5147-9507
Mitsuhiro A. Ishii: https://orcid.org/0000-0001-5282-8342
Binbin Cheng: https://orcid.org/0000-0002-8157-0982
Auke B.C. Otten: https://orcid.org/0000-0001-5034-9743
Bryan K. Sun: https://orcid.org/0000-0002-0740-0125

CONFLICT OF INTEREST

The authors state no conflict of interest.

ACKNOWLEDGMENTS

Research reported in this publication was supported by the National Institute on Arthritis and Musculoskeletal and Skin Diseases of the National Institutes of Health under award no. K08AR067853 to BKS.

AUTHOR CONTRIBUTIONS

Conceptualization: SYC, BKS; Data Curation: SYC, BKS, ABCO; Formal Analysis: SYC, BKS, ABCO; Funding Acquisition: BKS; Investigation: SYC, MAI, BC; Methodology: BKS, SYC, MAI, BC, ABCO; Resources: BKS; Supervision: BKS;

Visualization: SYC, BKS; Writing - Original Draft Preparation: SYC, BKS; Writing - Review and Editing, SYC, BKS, MA, BC, ABCO.

***Selena Y. Chen*[1], *Mitsuhiro A. Ishii*[1], *Binbin Cheng*[1], *Auke B.C. Otten*[1] and *Bryan K. Sun*[1,*]**

[1]*Department of Dermatology, University of California–San Diego, La Jolla, California, USA*

[*]*Corresponding author e-mail: bryansun@ucsd.edu*

SUPPLEMENTARY MATERIAL

Supplementary material is linked to the online version of the paper at www.jidonline.org, and at https://doi.org/10.1016/j.jid.2019.03.1141.

REFERENCES

Bürglin TR, Affolter M. Homeodomain proteins: an update. Chromosoma 2016;125:497–521.

Chen F, Kook H, Milewski R, Gitler AD, Lu MM, Li J, et al. *Hop* is an unusual homeobox gene that modulates cardiac development. Cell 2002;110:713–23.

Kee HJ, Kim J-R, Nam K-I, Park HY, Shin S, Kim JC, et al. Enhancer of polycomb1, a novel homeodomain only protein-binding partner, induces skeletal muscle differentiation. J Biol Chem 2007;282:7700–9.

Li B, Tsoi LC, Swindell WR, Gudjonsson JE, Tejasvi T, Johnston A, et al. Transcriptome analysis of psoriasis in a large case-control sample: RNA-seq provides insights into disease mechanisms. J Invest Dermatol 2014;134:1828–38.

Lopez-Pajares V, Qu K, Zhang J, Webster DE, Barajas BC, Siprashvili Z, et al. lncRNA-MAF: MAFB transcription factor network regulates epidermal differentiation. Dev Cell 2015;32:693–706.

Mariotto A, Pavlova O, Park H-S, Huber M, Hohl D. HOPX: the unusual homeodomain-containing protein. J Invest Dermatol 2016;136:905–11.

Mi H, Muruganujan A, Casagrande JT, Thomas PD. Large-scale gene function analysis with the PANTHER classification system. Nat Protoc 2013;8:1551–66.

Obarzanek-Fojt M, Favre B, Kypriotou M, Ryser S, Huber M, Hohl D. Homeodomain-only protein HOP is a novel modulator of late differentiation in keratinocytes. Eur J Cell Biol 2011;90:279–90.

Sen GL, Boxer LD, Webster DE, Bussat RT, Qu K, Zarnegar BJ, et al. ZNF750 is a p63 target gene that induces KLF4 to drive terminal epidermal differentiation. Dev Cell 2012;22:669–77.

Yang J-M, Sim SM, Kim H-Y, Park GT. Expression of the homeobox gene, HOPX, is modulated by cell differentiation in human keratinocytes and is involved in the expression of differentiation markers. Eur J Cell Biol 2010;89:537–46.

Yin Z, Gonzales L, Kolla V, Rath N, Zhang Y, Lu MM, et al. Hop functions downstream of Nkx2.1 and GATA6 to mediate HDAC-dependent negative regulation of pulmonary gene expression. Am J Physiol Lung Cell Mol Physiol 2006;291:L191–9.

Genome-Wide Association Study in Irradiated Childhood Cancer Survivors Identifies *HTR2A* for Subsequent Basal Cell Carcinoma

Journal of Investigative Dermatology (2019) **139,** 2042–2045; doi:10.1016/j.jid.2019.02.029

TO THE EDITOR

Survivors of childhood cancer are at increased risk for a variety of treatment-related complications and premature mortality (Armstrong et al., 2016), including subsequent neoplasms (SNs) (Bhatia and Sklar, 2002; Hudson et al., 2013; Olsen et al., 2009; Reulen et al., 2011). The Childhood Cancer Survivor Study (CCSS) (Friedman et al., 2010; Turcotte et al., 2017) previously showed that the risk of SNs increases with time from primary cancer diagnosis, yielding a 30-year cumulative incidence of 7.9% for subsequent malignant neoplasms and 9.1% for nonmelanoma skin cancer. Basal cell carcinoma (BCC) accounts for more than 80% of the nonmelanoma skin cancer cases (Watt et al., 2012), contributing to increased morbidity, impaired quality of life, and increased risk of subsequent cancer (Song et al., 2013).

Therapeutic irradiation is the most significant risk factor for BCC as a subsequent malignancy in childhood cancer survivors, with a well-established dose-response relationship (Watt et al., 2012). In contrast, incident BCC cases in the general population are strongly associated with sun exposure and skin color (Koh et al., 1996). Although it is clear that irradiated survivors of childhood cancer are at increased risk of BCC, many are exposed to radiotherapy but do not develop BCC. This interindividual variability despite the common risk-elevating exposure suggests a potential role of genetic susceptibility to subsequent BCC among survivors. To this end, we performed a genome-wide association (GWA) study of subsequent BCC among irradiated survivors of European ancestry in the CCSS discovery cohort (401 case patients and 2,330 control individuals) and evaluated genome-wide significant ($P < 5 \times 10^{-8}$) single-nucleotide polymorphisms (SNPs) in an independent cohort of irradiated long-term childhood cancer survivors (97 case patients and 1,082 control individuals) from the St. Jude Lifetime Cohort (i.e., SJLIFE). The institutional review boards at St. Jude Children's Research Hospital and at each of the CCSS participating centers approved the study, and participants provided written informed consent. Demographic characteristics of both cohorts are summarized in Supplementary Table S1 online.

We first examined associations between relevant nongenetic risk factors including sex, age at cancer diagnosis, attained age, primary cancer type and radiation exposures, and first BCC in the CCSS discovery cohort (see Supplementary Materials). The results of the multivariable clinical model (without any genetic variables) showed

Abbreviations: BCC, basal cell carcinoma; CCSS, Childhood Cancer Survivor Study; GWA, genome-wide association; HR, hazard ratio; MAF, minor allele frequency; SN, subsequent neoplasm; SNP, single nucleotide polymorphism

Accepted manuscript published online 22 March 2019; corrected proof published online 14 May 2019

SUPPLEMENTARY MATERIALS AND METHODS

Cell culture and treatment

Normal primary human keratinocytes were isolated from discarded neonatal foreskin from circumcisions and cultured in a 50:50 mixture of 154 Medium and KSFM Medium (Life Technologies, Waltham, MA) with manufacturer supplements, as well as penicillin/streptomycin and amphotericin. Differentiation was induced by plating cells to confluence and supplementing media with 1.2 mmol/L calcium.

Antibodies and reagents

The following commercial antibodies and dilutions were used for immunoblotting: HOPX (Santa Cruz Biotechnology, Dallas, TX; SC-30216) (1:250), HA (Cell Signaling, Danvers, MA; 3724) (1:1,000), ZNF750 (Proteintech, Rosemont, IL; 21752-1-AP) (1:200), β-tubulin (Developmental Studies Hybridoma Bank, Iowa City, IA; E7) (1:1,000−2,000), and β-actin (Sigma-Aldrich, St. Louis, MO; A1978) (1:1,000−4,000). Secondary antibodies included IRDye 800CW anti-rabbit (Li-Cor Biosciences, 926-32211) (1:10,000), IRDye 680RD anti-rabbit (Li-Cor Biosciences, 925-68071) (1:10,000), IRDye 800CW anti-mouse (Li-Cor Biosciences, 925-32212) (1:10,000), and IRDye 680RD anti-mouse (Li-Cor Biosciences, 926-68072) (1:10,000). The following commercial antibodies were used for immunofluorescence staining: LOR (Covance, Princeton, NJ; PRB-145P) (1:500), KRT10 (Abcam, Cambridge, UK; ab76318) (1:1,000−2,000). The secondary antibody was Alexa Fluor 555 anti-rabbit (Invitrogen, Waltham, MA; A21428) (1:500).

Western blotting

Keratinocytes were washed with cold phosphate-buffered saline (PBS), and protein lysate was extracted with RIPA buffer supplemented with protease inhibitor cocktail (Roche, Basel, Switzerland). Protein quantification was performed with a BCA Protein Assay kit (Pierce, Rockford, IL) following the manufacturer's instructions. Next, 12 μg of protein was resolved on 4%−12% SDS-PAGE gels (Invitrogen) with 2-(*N*-morpholino) ethanesulfonic acid (i.e., MES) buffer and transferred to nitrocellulose membranes. Membranes were incubated with primary antibodies overnight at 4 °C, washed three times in PBS-Tween (PBS-T), then incubated with secondary antibodies according to the manufacturer's recommendations (Li-Cor Biosciences). Detection of bands and quantitation was performed with Odyssey Image Analysis on the Odyssey Infrared Imager (Li-Cor Biosciences).

Immunofluorescence staining

Slides were fixed for 10 minutes by using 4% paraformaldehyde (for KRT10) or ice-cold acetone (for LOR), then permeabilized three times in PBS-T for at least 3 minutes each. Blocking was performed with blocking reagent (PBS-T, 5% goat serum) for 1 hour at room temperature and primary antibodies were incubated in PBS-T and 2% goat serum overnight at 4 °C. Slides were washed three times with PBS-T and incubated with secondary antibodies in 0.1% PBS-T and 2% goat serum for 45 minutes at room temperature. Slides were washed three times in PBS, then incubated with Hoechst stain for 2 minutes at room temperature, and washed with PBS twice and then with milli-Q water before mounting and visualization.

RNA interference

Short hairpin sequences were as follows: shHOPX: GTCAGCCAGCCC AGCTATTTA; HOPX shB: GCTAGCTG TCCTGCTGTTTAA; shZNF750: GGA AAGCCCTTCAAGTATAAA. Hairpins were cloned into the pLKO.1 cloning vector (available from Addgene, Watertown, MA) for lentiviral production.

Organotypic skin culture

Organotypic skin culture was performed essentially as described (Oh et al., 2013). Briefly, devitalized dermis was sectioned into 1.5 × 1.5-cm squares. Keratinocytes were seeded on the basement membrane of devitalized dermis and grown at the air-liquid interface for 7 days. Tissue was harvested and bisected: half was sectioned onto glass slides in 7-μm sections, and the other half was harvested for RNA.

Reverse transcription and quantitative real-time PCR

Total RNA was isolated with the Direct-zol RNA MiniPrep kit (Zymo Research, Irvine, CA), following the manufacturer's instructions. cDNA was synthesized from 500 ng of RNA with the iScript Reverse Transcriptase kit (Bio-Rad), and quantitative PCR performed with iTaq Universal SYBR Green Supermix (Bio-Rad). Real-time quantitative PCR was performed on a CFX96 Touch Real-Time PCR Detection System (Bio-Rad). For analysis of mRNA expression, the following primers were used: HOPX, 5′-CTTGCCTTTGCCTC TTCCAC-3′ and 5′-ACAGCCCAGGAA AATGAGCA-3′; loricrin, 5′-CCGGTGG GAGCGTCAAGT-3′ and 5′-AGGAGC CGCCGCTAGAGAC-3′; LCE3D, 5′-TTT CCTGTGGAAGGTCTGAGC-3′ and 5′-TGAGGTCAGGCACAAGCACT-3′; keratin 1, 5′-GCTGCAAGTTGTCAAGTT-3′ and 5′-TACCTCCACTAGAACCCAT-3′; keratin 10, 5′-AGCTATGGAAGTAGCA GCTTTGGTG-3′ and 5′-TCTGGCGCA GAGCTACCTCAT-3′; RPL32, 5′-AGGC ATTGACAACAGGGTTC-3′ and 5′-GTT GCACATCAGCAGCACTT-3′. RPL32 served as the loading control in all quantitative real-time reverse transcriptase−PCR analyses.

Cas9-expressing keratinocyte cell line

To generate a Cas9-expressing keratinocyte cell line, the Cas9-Flag-P2A-puromycin cassette was removed from the pLentiCRISPRv2 plasmid (Addgene, no. 52961) and cloned into the BamHI/XhoI sites of the pLEX MCS vector (Thermo Fisher Scientific, Waltham, MA). Next, the puromycin resistance cassette was swapped for a blasticidin resistance cassette, yielding the vector pLEX-Cas9-Blast. Lentivirus was generated with pLEX-Cas9-Blast and infected into the clone 103 keratinocyte cell line (Sun et al., 2015). After selection in 2 μg/ml of blasticidin for 3 days, selected keratinocytes were plated at 300 cells per 10-cm plate to allow expansion and isolation of individual keratinocyte clones. After 15−18 days of expansion, cell colonies were isolated by ring cloning and further expanded. Western blot was performed with the FLAG tag to identify candidate clones with the highest levels of Cas9 expression. Clone 10 (herein referred to as

103-Cas9-clone#10) was used for the subsequent CRISPR experiments.

CRISPR-Cas9 enhancer knockout

sgRNAs were designed to generate a loss-of-function deletion of the candidate enhancer downstream of the HOPX gene with the following sgRNA sequences: HOPXenh sgRNA-1, 5′-GAGCCACAGCTTATATTGGCA-3′; HOPXenh sgRNA-2, 5′-GCCTGGGATAGTGACCCTAAG-3′. The 103-Cas9-clone#10 keratinocytes were infected with lentivirus expressing scramble control sgRNA or HOPXenh sgRNA-1 and -2. Cells were selected with puromycin and differentiated with calcium for 6 days. Genomic DNA was isolated and the target genomic region amplified by using the following primers: HOPX-flank, 5′-TAGACTTTAGACACGCAGCCA-3′ and 5′-TTTCCCATGATGGACGTGCTA-3′. Amplicons were resolved on a 1.5% agarose gel.

HOPX and ZNF750 overexpression

The open reading frames of HOPX and ZNF750 were cloned in-frame with a 3′ hemagglutinin tag (HA) into the pLEX lentivirus vector (Thermo Fisher Scientific). Keratinocytes were infected with overexpression or empty vector, selected with puromycin, and evaluated for overexpression by Western blot against the HA tag. It was observed that the sgControl/sgEnhancer keratinocytes infected with empty vector or ZNF750 overexpression (Figure 1h) displayed impairment in up-regulating differentiation markers, which was attributed to having undergone multiple serial rounds of lentiviral infection and antibiotic selection. Therefore, to assess the impact on HOPX expression, differentiation in these cells was induced by short-term propagation at higher densities before harvesting.

RNA sequencing

Primary keratinocytes were infected with shCTRL or shHOPX in triplicate, selected with puromycin for 2 days, and then differentiated for 6 days in confluent conditions in the presence of 1.2 mmol/L calcium. Total RNA from shCTRL and shHOPX keratinocytes were subjected to RNA sequencing with the BGI-seq platform (BGI-America, Cambridge, MA). Quality control, genome alignment, and DEGs were analyzed with Partek Flow version 7.0 (Partek, St. Louis, MO). All samples had a read length of 100 base pairs with a minimal Phred quality score of 34. Reads were aligned to the human genome hg19 reference index with STAR, version 2.5.3a, with default settings (Dobin et al., 2013), resulting in more than 50 million aligned reads per sample. Aligned reads were quantified to hg19-RefSeq Transcripts, version 87, by using the Partek expectation/maximization method. Raw reads were normalized to the total number of counts per million reads. Normalized counts were analyzed for differential expression with an analysis of variance algorithm. Low-expressed genes were excluded if all samples had fewer than 5 reads. Genes were considered differentially expressed if there was at least a 2-fold difference in expression between control and HOPX knockdown and the false discovery rate was less than 0.01. Gene Ontology biological process analysis of the DEGs was performed with PANTHER (Mi et al., 2013) by using the Fisher exact test.

Band quantitation

Intensity of bands was quantitated with Image Lab Software analysis (Bio-Rad). Channel lanes and bands in the agarose gel were detected, and background signal was corrected. Band intensities were normalized to the amplicon length, and relative quantitation of bands was performed to generate a relative quantitation analysis table. Relative band quantitation was determined by the ratio of the band volume divided by the reference band volume.

Data availability statement

Data sets related to this article can be found at https://www.ncbi.nlm.nih.gov/geo/query/acc.cgi?acc=GSE125152, hosted at National Center for Biotechnology Information Gene Expression Omnibus under accession no. GSE125152.

SUPPLEMENTARY REFERENCES

Dobin A, Davis CA, Schlesinger F, Drenkow J, Zaleski C, Jha S, et al. STAR: ultrafast universal RNA-seq aligner. Bioinformatics 2013;29:15–21.

Mi H, Muruganujan A, Casagrande JT, Thomas PD. Large-scale gene function analysis with the PANTHER classification system. Nat Protoc 2013;8:1551–66.

Oh JW, Hsi TC, Fernando C, Ramos R, Plikus MV. Organotypic skin culture. J Invest Dermatol 2013;133(11):e14.

Sun BK, Boxer LD, Ransohoff JD, Siprashvili Z, Qu K, Lopez-Pajares V, et al. CALML5 is a ZNF750-and TINCR-induced protein that binds stratifin to regulate epidermal differentiation. Genes Dev 2015;29:2225–30.